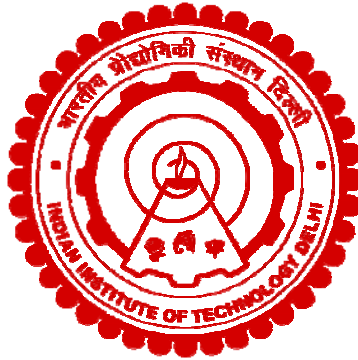


**SPINTRONIC-OSCILLATOR-BASED NEUROMORPHIC AND
ISING COMPUTING**

NEHA



**DEPARTMENT OF PHYSICS
INDIAN INSTITUTE OF TECHNOLOGY DELHI
JULY 2025**

© Indian Institute of Technology Delhi (IITD), New Delhi, 2025

**SPINTRONIC-OSCILLATOR-BASED NEUROMORPHIC AND
ISING COMPUTING**

by

NEHA GARG

Department of Physics

Submitted

in fulfillment of the requirements for the degree of Doctor of Philosophy

to the



INDIAN INSTITUTE OF TECHNOLOGY DELHI

JULY 2025

Certificate

This is to certify that the thesis entitled **Spintronic Oscillators based Neuromorphic and Ising Computing**, is being submitted by **Ms. Neha** to the Department of Physics, Indian Institute of Technology Delhi, for the award of the degree of **Doctor of Philosophy**. This work is a record of bona fide research conducted by him. He has worked under my supervision and guidance and has fulfilled all the requirements for the submission of this thesis. In my opinion, the work has reached the requisite standard.

The results presented in this thesis have not been submitted, either in part or in full, to any other university or institute for the award of any degree or diploma.

Prof. P. K. Muduli

Professor

Department of Physics

Indian Institute of Technology Delhi

New Delhi - 110016

India,

Date:

Prof. Debanjan Bhowmik

Associate Professor

Department of Electrical Engineering

Indian Institute of Technology Bombay

Mumbai - 400076

India,

Date:

Acknowledgements

This work represents the culmination of my unforgettable five-year Ph.D. journey. The successful completion of this research would not have been possible without the invaluable contributions of many individuals.

First, I sincerely thank my Ph.D. supervisors, Prof. Debanjan Bhowmik and Prof. Pranaba Kishor Muduli, for their invaluable support and guidance. Their belief in me, even when my efforts did not yield immediate results, gave me the strength and motivation to persevere. I greatly appreciate their patience, encouragement, and trust, which have been instrumental in helping me navigate challenges and grow both as a researcher and as an individual. I appreciate their willingness to dedicate time from their busy schedule for our discussions, which greatly enhanced my knowledge and curiosity about the latest developments in our field. I would like to give special thanks to Prof. Debanjan Bhowmik for engaging in various online meetings during Covid time, which gave a kickstart to my research. I sincerely appreciate his ability to critically analyze my results, consistently extracting meaningful insights and valuable contributions, even from the data that was quite inconclusive from my point of view. Without his unwavering support, I would not have been able to successfully complete my Ph.D. in the challenging and dynamic field of neuromorphic and Ising computing.

I extend my gratitude to the members of the SRC committee, Prof. Sujeet Chaudhary, Prof. Pintu Das, and Prof. Ankur Goswami, for their continuous feedback, invaluable insights, and engaging discussions during my Ph.D. tenure.

I am grateful to the Physics Department and High-Performance Computing (HPC) at IIT Delhi for providing the necessary software and computing. I would also like to acknowledge the University Grant Commission (UGC) for providing financial support throughout my research journey.

I thank all my senior labmates for fostering a welcoming environment since the beginning of my research journey. I express my appreciation to Dr. Naveen Sisodia for teaching me the fundamentals of micromagnetic simulations during the COVID-19 lockdown. This not only helped me use my time efficiently but also provided a kickstart to my Ph.D. I would like to thank Dr. Niru Chowdhury and Dr. Akash Kumar for their unwavering help and support. Dr. Kacho Imtiyaz Ali Khan, Pankhuri Gupta, Dr. Himanshu, Dr. Rekha Agarwal, and Richa Mudgal deserve my thanks for their contributions to engaging discussions throughout my Ph.D. tenure. Special thanks to Ram Singh Yadav for his assistance in making various corrections to my thesis. I also acknowledge and

thank all my juniors, including Nidhi Kandwal, Aman Saxena, and Vaishali Yadav.

I am deeply grateful to my friends, including Aman Sharma, Tamanna Punia, Arun Kumar Jaiswal, and Deeksha Gupta. They have played an instrumental role in making my Ph.D. journey truly memorable. The moments we have shared will be cherished for the rest of my life.

Finally, I would like to extend my heartfelt gratitude to my parents and extended family. Even on my worst days, their unwavering encouragement, unconditional love, and unrelenting support have been the driving force behind my journey. None of this would have been possible without their blessings and enduring support. I owe my presence here to the sacrifices of my parents and their tireless efforts to pave the way for a brighter future. They have consistently provided me with support and invaluable wisdom throughout my life.

This thesis is dedicated to my mother.

Neha

Abstract

Spintronic-oscillator-based computing has emerged as a promising technology for advancing neuromorphic and Ising computing due to its unique advantages, such as low power consumption, high scalability, and intrinsic nonlinearity. In neuromorphic computing, spintronic oscillators mimic the dynamics of biological neurons by using their tunable frequency, phase, and synchronization properties to perform various data classifications. Their high-speed operation offers significant potential for energy-efficient pattern recognition and machine learning tasks. For Ising computing, networks of coupled spintronic oscillators efficiently solve complex combinatorial optimization problems by emulating the energy minimization dynamics of spin systems. The inherent stochasticity and mutual coupling of these oscillators enable robust exploration of solution landscapes, making them well-suited for applications such as graph optimization, scheduling, and machine learning.

In the first part of the thesis, we explore the neuromorphic applications of spintronic oscillators. Firstly, we study the synchronization of a single oscillator with an external RF field and carry out the data classification. Next, we propose the hardware implementation of a Kuramoto-model-based data classification scheme through an array of dipole-coupled uniform-mode spin Hall nano-oscillators (SHNOs). Using micromagnetic simulations, which capture the underlying physics of the operation of the SHNOs, we first study the variation of synchronization range between two uniform-mode SHNOs as a function of the physical distance between them. Thus we correlate the coupling constant in the Kuramoto model with the dipole-coupling strength between two SHNOs, which our micromagnetic simulation takes into account. Next, we generate the synchronization map for the two-input-two-output dipole-coupled uniform-mode SHNO system through micromagnetics and show that it matches the one predicted by the Kuramoto model. Thus, we demonstrate here that the synchronization behavior of SHNOs obtained from micromagnetics-based modeling is consistent with that obtained from the Kuramoto model, which ignores the underlying physics of the SHNOs. This suggests that the Kuramoto-model-based data classification scheme can indeed be implemented physically on an array of SHNOs. To verify our claim, we show, through micromagnetic simulation, binary classification of data from a popular machine-learning data set (Fisher's Iris data set) using an array of uniform-mode SHNOs.

We then model the four-SHNO system (simulated through micromagnetics) using the single-domain magnetic model, or the macrospin model. For this purpose, we write down the Landau Lifschitz Gilbert Slonczweski (LLGS) equations for the precessing macrospin vectors representing the SHNOs, with the RF dipole field generated by macrospins introduced as an effective magnetic field

in the LLGS equation for the other macrospin, to take care of the coupling. We numerically solve these equations and present our results to show that they are consistent with the micromagnetic-simulation-based results and the Kuramoto-model-based results presented in the thesis. Solving the LLGS-equation-based single-domain model numerically is computationally much less resource-intensive compared to micromagnetic simulation because the dynamics of only one magnetization vector (the macrospin vector) is solved for here per SHNO, as opposed to that of numerous magnetic-moment vectors solved for in the micromagnetic method. Thus we establish that using a numerical method that is computationally very simple, we can also demonstrate that the dipole-coupled SHNOs follow the Kuramoto model, which is the main objective of the first part of the thesis.

In the second part of the thesis, we solve certain combinatorial optimization problems (COP), like Max-Cut. Solving COPs becomes challenging once the graph size and edge connectivity increase beyond a threshold, with brute-force algorithms that solve such problems exactly on conventional digital computers having the bottleneck of exponential time complexity. Hence, currently, such problems are instead solved approximately using algorithms like the Goemans-Williamson (GW) algorithm, run on conventional computers with polynomial time complexity. Phase binarized oscillators (PBOs), also often known as oscillator Ising machines (OIM), have been proposed as an alternative to solve such problems. In this thesis, restricting ourselves to the combinatorial optimization problem Max-Cut solved on three kinds of graphs (Mobius Ladder, random cubic, Erdős Rényi) up to 100 nodes, we empirically show that computation time/time to solution (TTS) for spintronic oscillators (captured through Slavin's model) grows at a much lower rate (logarithmically: $O(\log(N))$, with respect to graph size N) compared to the GW algorithm, for which TTS increases as the square of graph size ($O(N^2)$). While their accuracy is comparable to that of GW, spintronic oscillators have improved time complexity over the GW algorithm. Large graphs are expected to compute Max-Cut values much faster than the GW algorithm, as well as other oscillators operating at lower frequencies while maintaining the same level of accuracy. We have further incorporated noise to verify the robustness of our model. The addition of noise does not affect the accuracy of our solutions, justifying the applicability of our model to larger graphs in practical applications.

Overall, this dissertation demonstrates the potential of spintronic oscillators for neuromorphic and Ising computing by leveraging their synchronization dynamics and energy-efficient properties. Our findings highlight their capability for real-world applications in data classification and combinatorial optimization.

सार

स्पिनट्रॉनिक-ऑसिलेटर-आधारित कंप्यूटिंग अपने अनूठे लाभों, जैसे कम बिजली की खपत, उच्च मापनीयता और आंतरिक गैर-रैखिकता के कारण न्यूरोमॉर्फिक और आइसिंग कंप्यूटिंग को आगे बढ़ाने के लिए एक आशाजनक तकनीक के रूप में उभरी है। न्यूरोमॉर्फिक कंप्यूटिंग में, स्पिनट्रॉनिक ऑसिलेटर विभिन्न डेटा वर्गीकरण करने के लिए अपनी ट्यूनेबल आवृत्ति, चरण और सिंक्रोनाइज़ेशन गुणों का उपयोग करके जैविक न्यूरोन्स की गतिशीलता की नकल करते हैं। उनका उच्च गति संचालन ऊर्जा-कुशल पैटर्न पहचान और मशीन लर्निंग कार्यों के लिए महत्वपूर्ण क्षमता प्रदान करता है। आइसिंग कंप्यूटिंग के लिए, युग्मित स्पिनट्रॉनिक ऑसिलेटर के नेटवर्क स्पिन सिस्टम की ऊर्जा न्यूनीकरण गतिशीलता का अनुकरण करके जटिल संयोजन अनुकूलन समस्याओं को कुशलतापूर्वक हल करते हैं। इन ऑसिलेटर की अंतर्निहित स्टोकैस्टिसिटी और पारस्परिक युग्मन समाधान परिदृश्यों की मजबूत खोज को सक्षम बनाता है, जिससे वे ग्राफ अनुकूलन, शेड्यूलिंग और मशीन लर्निंग जैसे अनुप्रयोगों के लिए उपयुक्त बन जाते हैं।

थीसिस के पहले भाग में, हम स्पिनट्रॉनिक ऑसिलेटर के न्यूरोमॉर्फिक अनुप्रयोगों का पता लगाते हैं।

सबसे पहले, हम एक बाहरी आरएफ क्षेत्र के साथ एक एकल ऑसिलेटर के सिंक्रोनाइज़ेशन का अध्ययन करते हैं और डेटा वर्गीकरण करते हैं। इसके बाद, हम द्विध्रुवीय-युग्मित समान-मोड स्पिन हॉल नैनो-ऑसिलेटर की एक सरणी के माध्यम से कुरामोटो-मॉडल-आधारित डेटा वर्गीकरण योजना के हार्डवेयर कार्यान्वयन का प्रस्ताव करते हैं। माइक्रोमैग्नेटिक सिमुलेशन का उपयोग करते हुए, जो संचालन के अंतर्निहित भौतिकी को कैप्चर करता है, हम पहले दो समान-मोड ऑसिलेटर के बीच सिंक्रोनाइज़ेशन रेंज के परिवर्तन का अध्ययन उनके बीच भौतिक दूरी के एक फ़ंक्शन के रूप में करते हैं। इस प्रकार हम कुरामोटो मॉडल में युग्मन स्थिरांक को दो ऑसिलेटर के बीच द्विध्रुवीय-युग्मन शक्ति के साथ सहसंबंधित करते हैं, जिसे हमारा माइक्रोमैग्नेटिक सिमुलेशन ध्यान में रखता है। इसके बाद, हम माइक्रोमैग्नेटिक्स के माध्यम से दो-इनपुट-दो-आउटपुट डिपोल-युग्मित यूनिफ़ॉर्म-मोड ऑसिलेटर सिस्टम के लिए सिंक्रोनाइज़ेशन मैप तैयार करते हैं और दिखाते हैं कि यह कुरामोटो मॉडल द्वारा भविष्यवाणी की गई मैप से मेल खाता है। इस प्रकार, हम यहाँ प्रदर्शित करते हैं कि माइक्रोमैग्नेटिक्स-आधारित मॉडलिंग से प्राप्त ऑसिलेटर का सिंक्रोनाइज़ेशन व्यवहार कुरामोटो मॉडल से प्राप्त सिंक्रोनाइज़ेशन व्यवहार के अनुरूप है, जो ऑसिलेटर के अंतर्निहित भौतिकी को अनदेखा करता है। यह सुझाव देता है कि कुरामोटो-मॉडल-आधारित डेटा वर्गीकरण योजना वास्तव में ऑसिलेटर की एक सरणी पर भौतिक रूप से लागू की जा सकती है। अपने दावे को सत्यापित करने के लिए, हम माइक्रोमैग्नेटिक सिमुलेशन के माध्यम से यूनिफ़ॉर्म-मोड ऑसिलेटर की एक सरणी का उपयोग करके एक लोकप्रिय मशीन-लर्निंग डेटा सेट (फ़िशर के आइरिस डेटा सेट) से डेटा का बाइनरी वर्गीकरण दिखाते हैं।

फिर हम सिंगल-डोमेन मॉडल या मैक्रोस्पिन मॉडल का उपयोग करके चार- ऑसिलेटर सिस्टम (माइक्रोमैग्नेटिक्स के माध्यम से सिमुलेटेड) को मॉडल करते हैं। इस उद्देश्य के लिए, हम ऑसिलेटर का प्रतिनिधित्व करने वाले प्रीसेसिंग मैक्रोस्पिन वेक्टर के लिए लैंडौ लिफ़्सचिटज़ गिल्बर्ट स्लोन्ज़वेस्की (एलएलजीएस) समीकरण लिखते हैं, जिसमें युग्मन का ध्यान रखने के लिए अन्य मैक्रोस्पिन के लिए एलएलजीएस समीकरण में एक प्रभावी चुंबकीय क्षेत्र के रूप में पेश किए गए मैक्रोस्पिन द्वारा उत्पन्न आरएफ द्विध्रुवीय क्षेत्र होता है। हम इन समीकरणों को संख्यात्मक रूप से हल करते हैं और अपने परिणाम प्रस्तुत करते हैं ताकि यह दिखाया जा सके कि वे माइक्रोमैग्नेटिक-सिमुलेशन-आधारित परिणामों और

थीसिस में प्रस्तुत कुरामोटो-मॉडल-आधारित परिणामों के अनुरूप हैं। एलएलजीएस-समीकरण-आधारित एकल-डोमेन मॉडल को संख्यात्मक रूप से हल करना माइक्रोमैग्नेटिक सिमुलेशन की तुलना में कम्प्यूटेशनली बहुत कम संसाधन-गहन है क्योंकि यहाँ प्रति ऑसिलेटर के लिए केवल एक मैग्नेटाइजेशन वेक्टर (मैक्रोस्पिन वेक्टर) की गतिशीलता को हल किया जाता है, जबकि माइक्रोमैग्नेटिक विधि में कई चुंबकीय-क्षण वेक्टरों को हल किया जाता है। इस प्रकार हम यह स्थापित करते हैं कि एक संख्यात्मक विधि का उपयोग करके जो कम्प्यूटेशनली बहुत सरल है, हम यह भी प्रदर्शित कर सकते हैं कि द्विध्रुवीय-युग्मित ऑसिलेटर कुरामोटो मॉडल का पालन करते हैं, जो थीसिस के पहले भाग का मुख्य उद्देश्य है।

थीसिस के दूसरे भाग में, हम कुछ कॉम्बिनेटरियल ऑप्टिमाइज़ेशन समस्याओं (सीओपी) को हल करते हैं, जैसे मैक्स-कट। सीओपी को हल करना चुनौतीपूर्ण हो जाता है जब ग्राफ का आकार और एज कनेक्टिविटी एक सीमा से अधिक बढ़ जाती है, ब्रूट-फोर्स एल्गोरिदम के साथ जो ऐसी समस्याओं को पारंपरिक डिजिटल कंप्यूटरों पर ठीक से हल करते हैं, जिनमें एक्सपोनेंशियल टाइम जटिलता की अड़चन होती है। इसलिए, वर्तमान में, ऐसी समस्याओं को पारंपरिक कंप्यूटरों पर बहुपद समय जटिलता के साथ चलाने वाले गोमेन्स-विलियमसन (जीडब्ल्यू) एल्गोरिदम जैसे एल्गोरिदम का उपयोग करके लगभग हल किया जाता है। चरण बाइनरी ऑसिलेटर (पीबीओ), जिन्हें अक्सर ऑसिलेटर आइसिंग मशीन (ओआईएम) के रूप में भी जाना जाता है, को ऐसी समस्याओं को हल करने के विकल्प के रूप में प्रस्तावित किया गया है। इस थीसिस में, खुद को तीन तरह के ग्राफ (मोबियस लैडर, रैंडम क्यूबिक, एडॉस रेनी) पर हल किए गए कॉम्बिनेटरियल ऑप्टिमाइज़ेशन समस्या मैक्स-कट तक सीमित रखते हुए, हम अनुभवजन्य रूप से दिखाते हैं कि स्पिनट्रॉनिक ऑसिलेटर (स्लाविन के मॉडल के माध्यम से कैप्चर किए गए) के लिए गणना समय/समाधान का समय (टीटीएस) जीडब्ल्यू एल्गोरिदम की तुलना में बहुत कम दर (लॉगरिदमिक रूप से: $O(\log(N))$), ग्राफ आकार N के संबंध में) बढ़ता है, जिसके लिए टीटीएस ग्राफ आकार ($O(N^2)$) के वर्ग के रूप में बढ़ता है। जबकि उनकी सटीकता जीडब्ल्यू के बराबर है, स्पिनट्रॉनिक ऑसिलेटर ने जीडब्ल्यू एल्गोरिदम पर समय जटिलता में सुधार किया है। बड़े ग्राफ से अधिकतम-कट मानों की गणना GW एल्गोरिदम की तुलना में बहुत तेज़ी से की जाती है, साथ ही सटीकता के समान स्तर को बनाए रखते हुए कम आवृत्तियों पर काम करने वाले अन्य ऑसिलेटर भी। हमने अपने मॉडल की मजबूती को सत्यापित करने के लिए शोर को और शामिल किया है। शोर को जोड़ने से हमारे समाधानों की सटीकता प्रभावित नहीं होती है, जो व्यावहारिक अनुप्रयोगों में बड़े ग्राफ के लिए हमारे मॉडल की प्रयोज्यता को उचित ठहराता है। कुल मिलाकर, यह शोध प्रबंध न्यूरोमॉर्फिक और आइसिंग कंप्यूटिंग के लिए स्पिनट्रॉनिक ऑसिलेटर की क्षमता को उनके सिंक्रोनाइज़ेशन डायनेमिक्स और ऊर्जा-कुशल गुणों का लाभ उठाकर प्रदर्शित करता है। हमारे निष्कर्ष डेटा वर्गीकरण और कॉम्बिनेटरियल ऑप्टिमाइज़ेशन समस्याओं में वास्तविक दुनिया के अनुप्रयोगों के लिए उनकी क्षमता को उजागर करते हैं।

Contents

Certificate	i
Acknowledgements	iv
Abstract	vi
List of Figures	xv
List of Tables	xix
1 Fundamentals of Spintronics and Unconventional Computing	1
1.1 Spintronics	1
1.2 Basic Concepts	2
1.2.1 Magnetization Dynamics	2
1.2.2 Simulation at Different Length Scales: Micromagnetic and Macrospin Models	3
1.2.3 Micromagnetic Model	3
1.2.4 Macrospin Model	4
1.2.5 Zeeman Interaction	4
1.2.6 Heisenberg Exchange Interaction	5

1.2.7	Spin Transfer Torque	5
1.2.8	Microwave Oscillator Using the STT Effect	6
1.3	Neuromorphic Computing	7
1.3.1	Conventional and Unconventional Computing	7
1.4	Various Data Sets Used in the Thesis	8
1.4.1	Wisconsin Breast Cancer (WBC) Data Set	9
1.4.2	Iris Data Set of Flowers	9
1.4.3	MNIST Data Set of Handwritten Digits	9
1.5	Data Classification	9
1.5.1	Structure of a Fully Connected Neural Network (FCNN)	9
1.5.2	Data Classification Model for Fruit Classification	11
1.6	Ising Machine/Ising Computing	12
1.6.1	Mapping to Combinatorial Optimization Problems	13
1.6.2	Oscillator-Based Ising Machine	14
1.7	Thesis Organization	14
2	Synchronization of Spin Hall Nano Oscillator (SHNO) with External RF Field for Neuromorphic Applications	17
2.1	Introduction	17
2.2	Micromagnetic Simulation of Uniform-Mode SHNO	18
2.3	Synchronization of SHNO to External RF Magnetic Field	21
2.4	Classification with an Array of Uniform-mode SHNOs	23
2.4.1	Dimensionality Reduction of Input to Design the Target Synchronization Pattern	23

2.4.2	Tuning the SHNOs' Frequencies to the Target Synchronization Pattern to Achieve Learning	25
2.5	Conclusion	29
3	Mutual Synchronization among SHNOs for Neuromorphic Applications	31
3.1	Introduction	31
3.1.1	Method: Kuramoto Model for Oscillators	32
3.1.2	Method: Micromagnetic Simulation of Dipole-Coupled SHNOs	33
3.2	Synchronization between Two Oscillators	34
3.2.1	Kuramoto Model	35
3.2.2	Micromagnetic Study	36
3.3	Synchronization Map for the Two-Input-Two-Output Oscillator System	39
3.3.1	Kuramoto Model	39
3.3.2	Micromagnetic Study	42
3.4	Data Classification Using an Array of Spin Hall Nano-Oscillators	44
3.5	Single-Domain Magnetic Modeling of the Coupled-SHNO System	49
3.5.1	Single-Domain/ Macrospin Modeling of the Auto-Oscillation of a Single SHNO	50
3.5.2	Single-Domain/ Macrospin Modeling of the Synchronization Dynamics of Two Coupled SHNOs	53
3.6	On-Chip Inference On an Array of SHNOs	57
3.7	Conclusions	60
4	Phase Binarization among Dipole-Coupled SHNOs for Ising Computing	63
4.1	Introduction	63

4.2	Modeling of an Array of Dipole-Coupled Spin Hall Nano-Oscillators (SHNOs)	64
4.3	Phase Dynamics of Four Oscillators: Comparing LLGS and Kuramoto Models	68
4.4	Conclusion	70
5	Improved Time Complexity for Oscillator Ising Machines Compared to a Popular Classical Optimization Algorithm for the Max-Cut Problem	71
5.1	Introduction	71
5.1.1	Our Contribution	72
5.2	Modeling of Oscillator Ising Machines (OIMs)	74
5.2.1	Slavin’s Model of Spin Oscillators	74
5.3	The Max-Cut Problem and Connection with Oscillator Models	76
5.3.1	Types of Graphs Used	78
5.4	Comparing Performance of OIMs with GW Algorithm	79
5.4.1	Accuracy of Solution	79
5.4.2	Computation Time/ Time to Solution (TTS)	82
5.5	Discussion	84
5.5.1	Role of Thermal Noise	84
5.5.2	Nature of Coupling between Spintronic Oscillators and Future Perspective	85
5.6	Conclusion	86
6	Summary and Future Plans	87
	Bibliography	91
	Publications	99

List of Figures

1.1	Dynamics of a magnetic moment under the influence of (a) precession term only. (b) damping term only. (c) both precession and damping terms.	2
1.2	(a) Representation of micromagnetic model showing spatial discretization of ferromagnets in small cuboidal cells. (b) Illustration of macrospin model where the magnetic moment of the entire ferromagnet is represented with a single giant spin.	4
1.3	Schematic of a trilayer structure showing STT effect.	6
1.4	Representation of (a) conventional computing. (b) unconventional computing.	8
1.5	Images showing a glimpse of (a) Wisconsin Breast Cancer data set. (b) Iris data set of flowers. (c) MNIST data set of handwritten digits. (Fig. source: Wikipedia)	9
1.6	Structure of a general Fully Connected Neural Network (FCNN)	10
1.7	Data classification algorithm to classify various types of fruits	11
1.8	A 4-node weighted graph on which the Max-Cut problem is modeled. The nodes are split into two groups, one containing spin-up and the other containing spin-down states. The curve partitioning the two is drawn along with the weights of the cut edges.	13
2.1	(a) Schematic of the spin Hall nano oscillator (SHNO), which we simulate micromagnetically. The direction of the charge current and that of the applied DC magnetic field (H_{app}) are also shown. z is the vertical/out-of-plane direction. (b) Variation of the natural/auto-oscillation frequency of the SHNO with the magnitude of the charge current density, as obtained from the micromagnetic simulation.	18

2.2	Different snapshots of the ferromagnetic layer of SHNO show that its magnetic moments oscillate at a natural frequency of 6.7 GHz, where t is any arbitrary time and T is the period of oscillation.	20
2.3	Synchronization of the oscillator with vertically applied external RF magnetic fields for three different current densities, which result in three different natural frequencies of the oscillator	22
2.4	Schematic of the system of SHNOs used here for data classification	24
2.5	Through the application of the versatile NCA technique, each input in (a) Wisconsin Breast Cancer (WBC), (b) Fisher’s Iris, and (c) MNIST data sets is transformed into two dimensions: Feature 1, Feature 2. Then Feature 2 is plotted against Feature 1 for each of the data sets to show clustering of the data in reduced dimensions. . .	25
2.6	The final synchronization pattern obtained after training. The oscillators (SHNOs) are suitably synchronized with the input frequencies (of RF magnetic field) to achieve learning for the data sets (a) WBC (b) Fisher’s iris (c) MNIST. The number of steps needed to achieve the final training/learning stage, shown here, is 150 for all these data sets.	26
2.7	Classification accuracy for different training data sets obtained from our uniform-mode-SHNO-based network.	26
2.8	Intermediate stages of training for Iris data set	27
3.1	Schematic of the two-input-two-output oscillator system along with the classification algorithm	32
3.2	Micromagnetic simulation: (a) An average of the in-plane component (in the x direction, Fig 3.1) of all the magnetic moments in a single SHNO ($\langle m_x \rangle$) as a function of time for in-plane charge-current density = $4.95 \times 10^{11} \text{ A/m}^2$ shows sinusoidal behavior, signifying that the magnetization precesses steadily about the out-of-plane/ vertical (z) axis (Fig. 3.1). FFT of this magnetization vs time plot yields a natural frequency of 6.5 GHz. (b) Natural frequency vs. charge current density characteristic of a single SHNO.	34
3.3	Kuramoto model of two oscillators	35
3.4	Micromagnetic simulations of two SHNOs	36

3.5	Micromagnetic simulation: (a) Variation of the instantaneous frequencies of the two oscillators, SHNO1 and SHNO2 (Fig. 3.4(a)) with the natural frequency of SHNO 2 (F_2) when the natural frequency of SHNO 1 (F_1) is kept constant at 6.70 GHz and the distance between the two oscillators is 200 nm. The variation obtained here is similar to that obtained from the Kuramoto model in Fig. 3.3b. (b) Variation of the synchronization range for different values of distance between the two oscillators.	37
3.6	Kuramoto model of four oscillators	40
3.7	Effect of the frequency difference between output oscillators on synchronization maps	41
3.8	Schematic and Micromagnetic Simulations of two-input-two-output oscillator system	43
3.9	Data samples belonging to Fisher’s Iris data set, after transformation using NCA technique from their original 4 dimensions to 2 dimensions	45
3.10	Schematic and micromagnetic simulations of four SHNOs	48
3.11	Single-domain/ macrospin simulation: (a) The in-plane component (in the x direction, Fig 3.1) of the giant macrospin vector for a single SHNO (m_x) as a function of time, for in-plane charge-current density = 4.24×10^{11} A/m ² , shows sinusoidal behavior, signifying that the macrospin vector precesses steadily around the out-of-plane/ vertical (z) axis (Fig. 3.1).	52
3.12	Single-domain/ macrospin simulation: (a) Natural frequency of a single SHNO as a function of in-plane charge current density characteristic for a single SHNO (b) Precession angle θ (angle between the macrospin vector and the z-axis) as a function of in-plane charge current density	53
3.13	Single-domain simulations of two SHNOs	56
3.14	Synchronization map of four SHNOs using single-domain	59
4.1	Schematic of the array of dipole-coupled SHNOs arranged in a square geometry .	65

4.2	For the oscillator array of Fig. 4.1, phase differences between oscillator 2 and oscillator 1 (red plot), oscillator 3 and oscillator 1 (green plot), and oscillator 4 and oscillator 1 (blue plot) are plotted here with respect to time as obtained from (a) the LLGS model of spin oscillator and (b) the Kuramoto model for generalized PBO.	68
4.3	Schematic of the array of dipole-coupled SHNOs arranged in a row	69
4.4	Concerning the oscillator array of Fig. 4.3(a), the phase difference between oscillator 2 and oscillator 1 (red plot), oscillator 3 and oscillator 1 (green plot), and oscillator 4 and oscillator 1 (blue plot) plotted here are functions of time as obtained from LLGS model of the spin oscillators. Partitioning of the graph depends upon whether phase differences are odd or even multiples of π . As seen from here, LLGS model yields correct graph partitioning and Max-Cut score (3.037), as shown in Fig. 4.3(b).	70
5.1	Schematic of the spin transfer torque nano oscillator (STNO) captured by Slavin's model [12] in this work. PL: pinned layer (the layer in which the magnetic moment is fixed). FL: free layer (the layer in which the magnetic moment M_F precesses about an axis at steady state: oscillation. H_e represents the applied magnetic field, while θ_e and ϕ_e represent the direction cosines. I_{DC} is the current that generates spin transfer torque and triggers magnetic oscillation. Γ_+ and Γ_- are defined in the text [21].	74
5.2	Various instances of the three kinds of graphs used in the research	76
5.3	Evolution of the phases of spintronic oscillators, modeled by Slavin's model, over time corresponding to the 20-node Mobius ladder (ML) graph shown in Fig. 5.2(a). The difference between the phase ϕ of every other oscillator (numbered 2 to 20) and the phase of oscillator 1 (ϕ_1), normalized by π , has been plotted. Based on the phase differences in the final stable state, the partitioning is obtained (as described in the text) which matches with that shown in Fig. 5.2(b). The time at which the final steady state is obtained is reported as time to solution (TTS).	77
5.4	Mean approximation ratio vs size of the graph for both generalized PBOs (Kuramoto model) and spintronic oscillators (Slavin's model) for three kinds of graphs	80

5.5	Best case approximation ratio vs size of the graph (in terms of number of nodes N) for both generalized PBOs (Kuramoto model) (green plot) and spintronic oscillators (Slavin's model) (red plot) and three kinds of graphs: (a) Mobius Ladder, (b) random cubic, (c) and Erdős Rényi. The method to calculate the best case approximation ratio is described in the text. To obtain this plot, no thermal noise has been incorporated in either Kuramoto's model or Slavin's model.	80
5.6	Time to solution (TTS), normalized by TTS for the same method for a graph instance of the same graph type with 10 nodes, vs size of the graph for generalized PBOs (Kuramoto model), spintronic oscillators (Slavin's model) and GW algorithm for three kinds of graphs	81
5.7	Evolution of the phases of spintronic oscillators, modeled by Slavin's model, over time corresponding to the 30-node Mobius ladder (ML) graph with and without noise	85

List of Tables

2.1	Comparison of classification accuracy numbers between the uniform-mode SHNO network and a standard single-layer perceptron/Fully Connected Neural Network without a hidden layer, trained in software.	28
3.1	Classification accuracy numbers for the three binary classification tasks within Fisher’s Iris data set as obtained from the synchronizaion maps in Fig. 3.9	47
5.1	Time to solution (TTS) for solving Max-Cut on graphs of 10 nodes using generalized PBOs (Kuramoto model), spintronic oscillators (Slavin’s model), and GW algorithm. Parameter values used, the value of each time step for PBOs, and specifications of the conventional computer on which GW algorithm is run for this work are mentioned in the text.	81
5.2	Comparison of cut values obtained from Slavin’s model of spin oscillators (without and with noise incorporated in them) for different cut values.	84